Available online at www.sciencedirect.com
SCIENCE DIRECT®
C. R. Chimie 8 (2005) 1093–1100
COMPTES RENDUS CHIMIE
http://france.elsevier.com/direct/CRAS2C/

$(\eta\text{-}X)_2[(\mu\text{-}S_2)M_2]$ complex cores (X = O, S; M = Mo^V, W^V): the *syn*/*anti* isomerism revisited by means of DFT calculations

Marie-Madeleine Rohmer *, Marc Bénard *

Laboratoire de chimie quantique, UMR 7551, CNRS, université Louis-Pasteur, 4, rue Blaise-Pascal, 67000 Strasbourg, France

Received 27 August 2004; accepted after revision 20 October 2004

Available online 08 February 2005

Abstract

A series of five sulfur-rich binuclear, di-anionic complexes involving the $(\eta\text{-}X)_2[(\mu\text{-}S_2)M_2]$ core (X = O, S; M = Mo^V, W^V), and completed with two dithiolene ligands, is investigated by means of Density Functional Theory (DFT). Geometries have been optimized, in order to address the problem of the *syn*/*anti* isomerism. It is found that the equilibrium geometry of all investigated systems in either conformation deviates from the expected full symmetry. This distortion, mainly affecting the dithiolene ligands, is assigned to the strong electrostatic and Pauli repulsion, which develops inside the coordination sphere of each metal. These repulsive interactions are shown to be of similar strength in the *syn* and *anti* forms *of the isolated molecules* and do not critically affect the energy balance between the two isomers. As suggested 23 years ago by Chandler, Lichtenberger and Enemark (CLE), the *bent σ bond* provides the *syn* form a slight advantage (1–4 kcal mol^{-1}) over the *lateral σ bond* characteristic of the *anti* isomer. It is expected that environmental effects and more specifically the location of the counterions are of crucial importance regarding the relief of the intramolecular repulsion and the relative stability of isomers in the crystal. ***To cite this article: M.-M. Rohmer et M. Bénard,C. R. Chimie 8 (2005).***

Résumé

Nous avons étudié, dans le cadre de la théorie de la fonctionnelle de la densité (DFT), une série de cinq complexes binucléaires et dianioniques centrés sur le cœur $(\eta\text{-}X)_2[(\mu\text{-}S_2)M_2]$ (X = O, S; M = Mo^V, W^V) et complétés par deux ligands dithiolènes. Les géométries ont été optimisées, dans le but de discuter le problème de l'isomérie *syn*/*anti*. Dans tous les systèmes étudiés, la conformation d'équilibre s'écarte de la symétrie maximale attendue. Cette distorsion, qui affecte en premier lieu les ligands dithiolènes, est attribuée aux fortes répulsions électrostatiques et de Pauli, qui affectent la sphère de coordination de chaque métal. On montre que ces répulsions sont d'intensité équivalente dans les formes *syn* et *anti* et n'affectent pas de façon déterminante l'équilibre énergétique entre les isomères. En accord avec l'hypothèse formulée voici 23 ans par Chandler, Lichtenberger et Enemark, il apparaît que la *liaison σ courbe* confère à la forme *syn* un léger avantage énergétique, compris entre 1 et 4 kcal mol^{-1}, sur le *recouvrement σ latéral* caractéristique de la forme *anti*. On s'attend néanmoins à ce que les facteurs d'environnement, et en particulier la nature et l'emplacement des contre-ions, aient une importance cruciale dans la gestion des

* Corresponding authors.
E-mail addresses: rohmer@quantix.u-strasbg.fr (M.-M. Rohmer), benard@quantix.u-strasbg.fr (M. Bénard).

1631-0748/$ - see front matter © 2005 Académie des sciences. Published by Elsevier SAS. All rights reserved.
doi:10.1016/j.crci.2004.10.017

répulsions intramoléculaires et dans la stabilité relative des isomères en phase cristalline. ***Pour citer cet article : M.-M. Rohmer et M. Bénard, C. R. Chimie 8 (2005).***

Keywords: DFT; Geometry optimization; *Syn*/*anti* isomerism; Sulfur-rich complexes; Bent metal–metal bond

Mots clés : DFT ; Optimisation de géométrie ; Isomérie *syn*/*anti* ; Complexes riches en soufre ; Liaison courbe métal–métal

1. Introduction

The reaction of tetraoxothiometalates $[MS_nO_{4-n}]^{x-}$ (M = V, Mo, Re, W) with electrophiles has been widely used in the last decade to produce a variety of sulfur-rich complexes of transition metals [1–8]. More specifically, the use of unsaturated substrates like alkynes as electrophilic agents has led to the preparation of new dithiolene ligands, eventually attached to metal cores with various nuclearities. Beyond mononuclear species [9–14], this synthetic pathway has contributed to enlarge and diversify the series of dianions organized around the $(\mu\text{-}S_2)M_2$ metallacycle, and completed with two monoatomic ligands, either oxo or sulfido [7,8,15–21]. The position of these two M=X bonds with respect to the metallacycle gives rise to the classical *syn/anti* isomerism, illustrated in Fig. 1 [20,21][1].

Most structures involving the $(\eta\text{-}X)_2[(\mu\text{-}S_2)M_2]$ core have been characterized in the *syn* form only [7,8,16–19]. Both the *syn* and the *anti* isomers have been isolated and characterized for the first time on a Mo^V dianionic complex with symmetric dithiolene ligands, $[Mo_2S_4(S_2C_2H_4)_2]^{2-}$ (**1**) [20]. Since then, various complexes have been characterized with both structures, including Mo^V complexes similar to **1** in which sulfido ligands have been replaced by oxo [8], and the series of bi- and tetranuclear compounds derived from ReS_4^- and synthesized by Goodman and Rauchfuss [15]. A theoretical analysis of the bonding in the *syn* and *anti* isomers of **1** was given by Chandler, Lichtenberger and Enemark (CLE) in 1981 [22], based upon Hall and Fenske [23] and extended Hückel (EHMO) [24–26] calculations. This study assigned the diamagnetism observed in both isomers to the presence of a metal–metal bond, "not large, but sufficient" to stabilize a closed-shell ground state [22]. The *syn* form was also predicted to be the most stable one, based on the calculated total energies and on the relative strength of the Mo–Mo bonding, estimated from the total Mo–Mo 4d overlap populations. A third, hypothetic form, the "closed" isomer, topologically equivalent to the *syn* form, but with a planar Mo_2S_2 metallacycle, was also investigated [22]. Even though the study by CLE was state of the art in 1981, its conclusions can hardly go beyond the qualitative aspects of the bonding, due to the lack of geometry optimization and to the crude estimates of total energies obtained from the above-mentioned semi-empirical methods. Quite recently, the bifunctional dithiolene $S_2C_2[C(O)OMe]_2$ was grafted on a $(\eta\text{-}X)_2[(\mu\text{-}S_2)W_2]$ core (X = O, S) by the group of Sécheresse, and resulted in complexes only displaying the *anti* conformation [27]. A subtle illustration of the *syn/anti* problem was also evidenced by the same group through the synthesis and X-ray characterization of a monovacant heteropolytungstate dimer in which the $(PW_{11}O_{39})^{7-}$ monomers are coupled through two $\{(\eta\text{-}O)_2(\eta\text{-}OH_2)_2[(\mu\text{-}S_2)Mo_2]\}^{2+}$ bridges [28]. The metal–oxo bonds of the bridges are subject to the *syn/anti* isomerism, but the presence of a disorder in the structure has prevented to support one arrangement over the other. The goal of the present work is therefore to obtain by means of Density Functional Theory (DFT) a reliable estimate of the energy difference between the *syn* and *anti* isomers in standard dithiolene complexes of Mo^V, and then to vary the models and the electronic configurations in order to obtain a detailed analysis of the electronic and electrostatic factors conditioning the relative stability of both isomers.

2. Computational details

Most calculations and all geometry optimizations reported in the present work have been carried out using

[1] Note that the crystal atomic coordinates provided for the anti isomer of 1 are in error for the dithiolene sulfur atoms S3 and S4. Crystal parameters consistent with the rest of the structure are as follows: S3: $x = 0.6603$; $y = 1.1454$; $z = 0.2015$, S4: $x = 0.4963$; $y = 0.9895$; $z = 0.3043$.

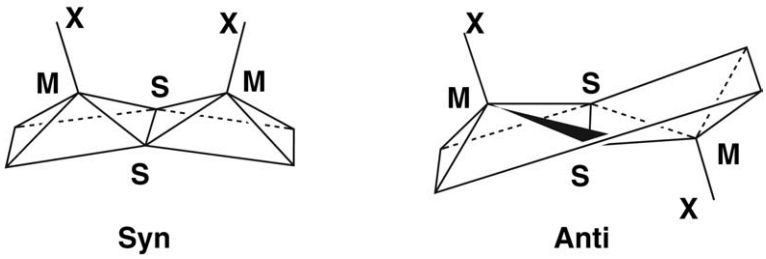

Fig. 1. Schematic representation of the ligand square pyramids in the *syn* and *anti* forms of $[M_2(\mu\text{-}S_2)X_2(S_2R)_2]^{2-}$.

the DFT formalism by means of the 1999 release of the ADF program, based upon the use of Slater basis sets [29–32]. The exchange-correlation functional is the so-called Becke–Perdew/86 (BP86) functional [33–35], which belongs to the family of functionals referring to the generalized gradient approximation (GGA). The atomic basis sets used in the present calculations are referred to in the User's Guide as TZP for H, C, O and S atoms, and TZ2P for Mo and W. These basis sets are to be used in conjunction with the Zero Order Regular Approximation (ZORA) to the relativistic effects with appropriate description of the inner shells, an option that was adopted throughout the present calculations. The atomic description consists in a core (He core for first-row atoms, Ne core for S, Kr and Xe cores for Mo and W, respectively) described by means of frozen double-ζ Slater functions. The valence shells are triple-ζ and supplemented either with one d-type polarization function (non-metal atoms) or with an extra p-type function and a f-type polarization function (Mo, W). Some calculations were also carried out with EHMO [24–26] in order to obtain qualitative orbital interaction diagrams.

3. Discussion

*3.1. The case of $[Mo_2S_4(S_2C_2H_4)_2]^{2-}$ (**1**) and $[Mo_2S_2O_2(S_2C_2H_4)_2]^{2-}$ (**2**)*

Complex **1** has been the subject of the theoretical investigation carried out by CLE [22]. Not surprisingly, EHMO calculations carried out on **1** and on its oxo counterpart **2** reproduce the sequence of frontier MOs obtained by CLE from the Fenske–Hall method. Fig. 2 displays the EHMO interaction diagram constructing the orbitals of the *syn* form of **2** from the molecular fragments $[Mo_2O_2(S_2C_2H_4)_2]^{2+}$ and $(\mu\text{-}S_2)^{4-}$. The HOMO of **2** results from the σ-bonding combination of the two ML_3 fragments. This orbital is somewhat destabilized due to a 4-electron interaction with $\mu\text{-}S_2$, but the energy increase remains moderate (Fig. 2). By contrast, electron donation from $\mu\text{-}S_2$ to the other metal levels significantly raises the energy of these unoccupied levels and generates a conspicuous HOMO–LUMO gap (1.35 eV). More specifically, the presence of the S_2 bridge raises by 50% the energy gap between the σ-bonding and the σ-antibonding Mo–Mo levels (Fig. 2). These donation interactions globally stabilize the set of six valence orbitals of $\mu\text{-}S_2$ and ensure the stability of the complex. The frontier orbitals of the *anti* isomer can be deduced from those of Fig. 2 by a 180° rotation of one Mo–oxo–dithiolene fragment. The energy difference between the σ and the σ* levels is reduced by ~30% in the *anti* Mo_2L_6 fragment, but the donation from $\mu\text{-}S_2$ restores an important energy gap and the sequence of frontier MOs is eventually quite similar to that of the *syn* isomer, with a slight raise of the HOMO energy (0.15 eV).

In view of these qualitative results, one might conclude in agreement with CLE that the relative stability of the *syn* and *anti* isomers should be correlated with a difference in the strength of the metal–metal bond, the relative orientation of the metal σ orbitals being more favorable in the *syn* conformation. This explanation seems in keeping with the slightly longer Mo–Mo distances observed for the *anti* forms, when both isomers are available [8,20]. However, one could also argue that the shortening of the Mo–Mo bond in the *syn* form is a mere consequence of the butterfly folding of the metallacycle rather than the parameter monitoring the relative stability of the system. Indeed, the Mo-(μ-S) distances, either observed or computed, remain quite similar in the bent metallacycle of the *syn* form, and in the planar core of the *anti* isomer (Table 1). One should also consider that the network of repulsive interactions

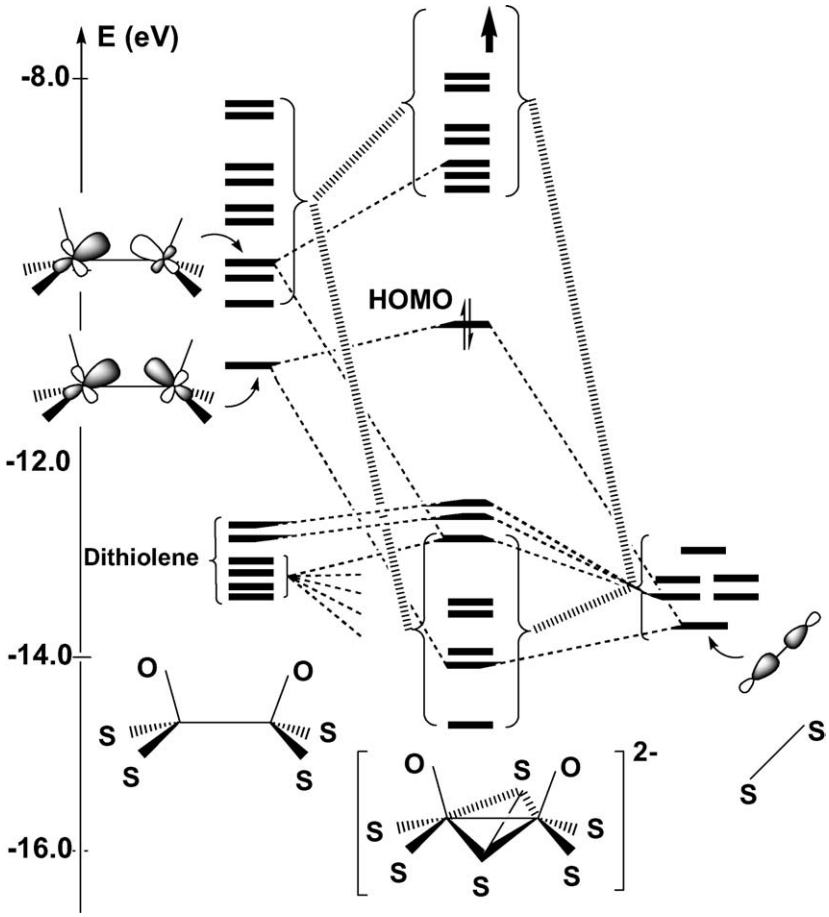

Fig. 2. Orbital interaction diagram for the *syn* form of $[Mo_2(\mu\text{-}S_2)O_2(S_2C_2H_4)_2]^{2-}$ from EHMO calculations.

developed among the highly charged ligands represents another factor that might influence the relative stability of the isomers. These repulsive contacts are partly accounted for by the EHMO interaction diagram in the form of repulsive 4-electron interactions occurring between the fragment orbitals of dithiolene and those of $\mu\text{-}S_2$ (Fig. 2). It is clear however that the Pauli and electrostatic components of this L–L repulsion are severely underestimated by EHMO. An opposite twist of the two dithiolene groups induced by a Θ rotation around their local symmetry axis is observed in some structures, the two forms of **1** [20] as well as in some other members of the same family of compounds [8]. This distortion reduces the molecular symmetry from C_{2v} to C_2 in the *syn* form, and from C_{2h} to C_i in the *anti* form (Fig. 3). A particular emphasis should be given to the *anti* isomer of **1**, a strongly distorted structure in which the twist angle reaches the relatively high value of 11.1° (Table 1). This deviation from ideal symmetry does not seem to be related to any specific interaction involving the frontier orbitals and could therefore be assigned either to the crystal forces, or to ligand–ligand repulsive interactions. One of the goals of the DFT calculations reported in the present work was to provide evidence for these interactions and to quantitatively assess their role in the energy balance between the *syn* and *anti* forms.

Table 1 displays the relative energies obtained for both isomers of **1** and **2** after gradient optimization of the geometries, together with the observed and calculated values of selected structural parameters. These calculations have been carried out assuming the C_2 symmetry for the *syn* form and the C_i symmetry for the *anti* form. The geometry of the same systems have also been

Table 1
Relative energies (ΔE, kcal mol^{-1}), selected bond lengths (Å), dihedral and twist angles (°) calculated for **1** and **2** and observed for **1**. Calculations carried out with symmetry constraints are also reported, together with the relative energies calculated in the constrained and unconstrained geometries for the $[Mo_2X_2(S_2C_2H_4)_2]^{2+}$ fragments

	1 *syn*			**1** *anti*			**2** *syn*		**2** *anti*	
	Calc.		*Obs.*	Calc.		*Obs.*	Calc.		Calc.	
	C_2	C_{2v}		C_i	C_{2h}		C_2	C_{2v}	C_i	C_{2h}
Dianion										
Mo–Mo	2.907	2.911	*2.863*	2.947	2.944	*2.878*	2.894	2.902	2.961	2.962
Mo–X	2.160	2.164	*2.098*[a]	2.171	2.170	*2.129*[a]	1.708	1.710	1.712	1.712
Mo-μS	2.350[a]	2.352	*2.320*[a]	2.345[a]	2.349	*2.321*[a]	2.363[a]	2.366	2.361[a]	2.365
Mo–S_{dith}	2.448[a]	2.430	*2.406*[a]	2.445[a]	2.427	*2.401*[a]	2.470[a]	2.451	2.466[a]	2.445
Θ[b]	6.3	0.0	*2.0*	6.4	0.0	*11.1*	4.7	0.0	7.4	0.0
Π[c]	144.5	147.8	*146.9*	180.0	180.0	*180.0*	143.6	145.8	180.0	180.0
ΔE	0.0	+7.3		+3.4	+11.5		0.0	+8.3	+3.9	+12.8
Dicationic fragment										
ΔE	+0.1	0.0		+3.8	+4.9		+0.05	0.0	+2.7	+3.1

[a] Average distance.
[b] Twist angle measuring the rotation of each S_{dith}–Mo–S_{dith} with respect to the position of perfect symmetry (Fig. 3).
[c] Dihedral angle between the two M-(μ-S_2) planes.

optimized with the more severe constraints of the C_{2v} and C_{2h} point groups, respectively, in order to provide a first estimate of the effects of L–L repulsion. Finally, single-point calculations have been carried out on the dimetallic complex *without* μ-S_2, assuming either the unconstrained or the constrained geometry for the $[Mo_2X_2(S_2C_2H_4)_2]^{2+}$ fragments (Table 1).

DFT calculations confirm that the *syn* isomers of **1** and **2** are more stable than their respective *anti* counterparts. The computed energy difference is of the order of 3.5 kcal mol^{-1} (Table 1). The observed geometrical parameters of **1** *syn* and **1** *anti* are well reproduced by the calculations, accounting for the slight overestimation (0.03–0.06 Å) of the metal–metal and metal–ligand bond lengths generally encountered with the GGA functionals. All distances are quite similar in the two isomers, except for the Mo–Mo bond length, which is found shorter in the *syn* form by 0.04 and 0.07 Å in **1** and **2**, respectively (Table 1). The butterfly folding of the metallacycle observed in **1** *syn* is well reproduced in the computed structure. Finally, the calculations show that the deviation from full symmetry induced by the twist of the dithiolene rings is an intrinsic character of the isolated molecule and contributes to its stability by as much as 7–9 kcal mol^{-1} for both isomers of **1** and **2** (Table 1). Note that the calculated interatomic distances are quite similar in the real and in the ideal symmetry, except for the average Mo–S_{dith} bond length which displays a small, but systematic contraction (~0.02 Å) in the most symmetric structure. In order to assess the role of ligand–ligand repulsive interactions in the dithiolene distortion, the energy of the $[Mo_2X_2(S_2C_2H_4)_2]^{2+}$ fragments obtained by removing (μ-S_2)$^{4-}$ from **1** and **2**, was computed by means of

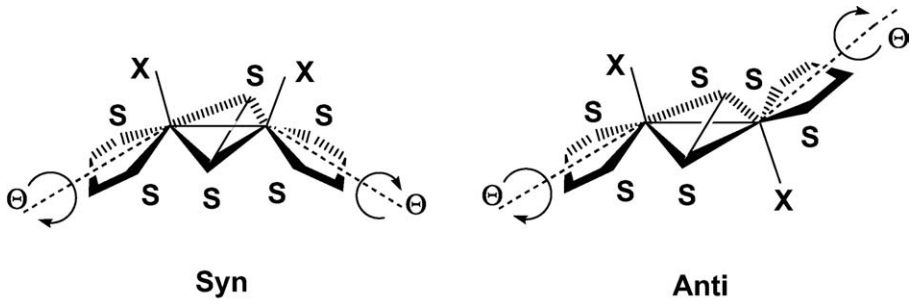

Fig. 3. Distortion of the dithiolene ligands downgrading the molecular symmetry of the *syn* and *anti* forms of $[Mo_2(\mu\text{-}S_2)X_2(S_2C_2H_4)_2]^{2-}$.

single-point calculations. The geometries were taken from those optimized for both isomers of **1** and **2**, assuming either the real, or the ideal symmetry (Table 1). Contrary to the case of the full complexes, the stability of the dicationic fragments is practically insensitive to the dithiolene twist. For both fragments, the *syn* form remains energetically favored by about the same amount (3–4 kcal mol^{-1}) as for the full complex (Table 1).

It can therefore be concluded that a relatively important repulsion develops between $(\mu\text{-}S_2)^{4-}$ and the rest of the coordination sphere of sulfur-rich dimetallic complexes. This repulsion is smoothed by downgrading the molecular symmetry as represented in Fig. 3, possibly at the expense of a slight decline in the strength of the $Mo–S_{dith}$ bond. However, it eventually appears that the ligand–ligand repulsion does not significantly affect the energy balance between the *syn* and *trans* isomers. The relative stability of the isolated dianionic structures, as that of the related dicationic fragments, therefore, remains ultimately conditioned by the different strength of the metal–metal σ-bond, either bent, in the *syn* form, or lateral, in the *trans* isomer (Fig. 4) [22].

3.2. Complexes of functionalized dithiolenes: $[M_2S_2X_2(S_2C_2R_2)_2]^{2-}$ (R = C(O)OMe; M = Mo, W)

More recently, the use of alkynes, and more specifically of dicarbomethoxyacetylene as reducing agent resulted in the synthesis of functionalized dithiolenes as ligands of the $(\eta\text{-}X)_2[(\mu\text{-}S_2)M_2]$ core. Coucouvanis et al. [8] reported the structure of both the *syn* and the *anti* isomers of $[Mo_2S_2O_2(SCC(O)OMe)_2]^{2-}$ (**3**). Very recently, the group of Sécheresse characterized similar compounds with M = W; X = O (**4**) and S (**5**), but the *anti* form only could be isolated and characterized up to now [27].

Calculations show that the *syn* form of the molybdenum oxo compounds **3** is again more stable than the *anti* isomer, although the energy difference is reduced to ~1 kcal mol^{-1} (Table 2). The structural parameters of the coordination sphere are not significantly different from those of the parent compound **2**, except for a more pronounced folding of the metallacycle. This folding contracts the Mo–Mo distance, which is computed shorter than in the *anti* form by 0.086 Å. This difference is the largest computed in the whole series of investigated complexes. The observed gap between the

Fig. 4. The metal–metal bonding in the *syn* and *anti* forms of $[M_2(\mu\text{-}S_2)X_2(S_2R)_2]^{2-}$.

Table 2
Relative energies (Δ*E*, kcal mol^{-1}), selected bond lengths (Å), dihedral and twist angles (°) calculated and observed for $\{M_2X_2S_2[S_2C_2–(COOMe)_2]_2\}^{2-}$ (**3**: M = Mo, X = O; **4**: M = W, X = S; **5**: M = W, X = O)

	3 *syn*		**3** *anti*		**4** *syn*	**4** *anti*		**5** *syn*	**5** *anti*	
	Calc.[d]	*Obs.*	Calc.[d]	*Obs.*	Calc.	Calc.	*Obs.*	Calc.	Calc.	*Obs.*
M–M	2.858	*2.853*	2.944	*2.904*	2.925	2.956	*2.869*	2.921	2.956	2.870
M–X	1.703	*1.675*	1.708	*1.684*	2.166	2.170	*2.090*	1.729	1.726	1.820
M-μS[a]	2.362	*2.331*	2.353	*2.328*	2.350	2.350	*2.314*	2.363	2.363	2.322
$M–S_{dith}$[a]	2.456	*2.425*	2.456	*2.419*	2.436	2.433	*2.395*	2.458	2.451	2.402
Θ[b]	5.8	*3.9*[a]	5.2	*1.0*	5.3	3.1	*1.3*	7.8	1.8	0.7
Π[c]	138.0	*148.0*	180.0	*180.0*	153.6	180.0	*180.0*	153.5	180.0	180.0
Δ*E*	0.0		+1.1		0.0		+3.6		0.0	+2.2

[a] As in Table 1.
[b] As in Table 1.
[c] As in Table 1.
[d] Calculations on **3** have been carried out on models in which the methoxy groups have been replaced by OH.

Mo–Mo bond lengths in the *syn* and *anti* forms of **3** amounts 0.051 Å, which is also much larger than observed for **1** (0.015 Å). However, no conspicuous correlation shows up in the series of complexes **1**–**5** between the relative stability of the *syn* form and the shrinkage of the metal–metal bond length in this isomer. Indeed, the contraction of the M–M distance is a purely geometrical consequence of the folding angle Π between the two M-(μ-S_2) planes and does not necessarily imply a better σ overlap between the metal atoms.

The replacement of Mo^V by W^V hardly modifies the M–S and M–X bond lengths, but opens the wings of the *syn* butterfly. The Π angle is calculated larger by 10 to 15° for the *syn* isomers of **4** and **5** than for the Mo complexes **1**–**3** (Tables 1 and 2). An immediate consequence is the reduction to ~0.035 Å of the M–M distance gap calculated between the *syn* and *anti* isomers. The geometrical origin of this wing opening is a less pronounced bending of the dithiolene rings with respect to the metal–metal axis. Even though no folding can occur in the *anti* form, a similar leveling of the square pyramid M–S_4 basis is observed and computed in the isomers with C_i symmetry. In keeping with this evolution of the molecular geometry, the ligand–ligand repulsion, as estimated by the twist angle *Θ*, tends to decrease, at least for the *anti* isomers. It is interesting to compare the computed values of *Θ* with the observed ones, when available in either form of complexes **1**–**5** (Table 2). With the notable exception of *anti*-**1**, the observed values of *Θ* are significantly lower than the computed ones. In the *anti* forms of **3**, **4** and **5**, the observed distortion even becomes almost negligible (~1°) when the computed values are comprised between 1.8° and 5.2°. It can be inferred that the crystal forces and more specifically the influence of the counter-ions tend in this case to oppose the repulsive interactions, whereas they seem to be enhanced in *anti*-**1**.

As for complexes **1** and **2** the *syn* form of **4** and **5** is more stable than the *anti* conformation by a few kcal mol^{-1}, as long as they are considered isolated (Table 2). At variance with the structures displayed in Table 1, the computed distortion of the dithiolene ligands is consistently more important in the *syn* form than in the *anti* form of **4** and **5**. This might influence the relative stability of the isomers: a secondary energy minimum, less distorted then the structure reported in Table 2, had been first characterized for **5** *syn* with an energy slightly higher than that calculated for **5** *anti* (+0.35 kcal mol^{-1}). Besides, the geometry optimization of the *anti* forms of **4** and **5** has been carried out starting from the little distorted X-ray structure as trial geometry. Therefore, it cannot be totally excluded that a more severe distortion of dithiolene provides further stabilization to the *anti* forms of these isolated complexes.

4. Summary and conclusion

DFT calculations carried out on binuclear di-anionic complexes of Mo^V or W^V with a square-pyramidal XMS_4 coordination environment provides some new information about the *syn*/*anti* isomerism, characteristic of these molecules. Rather surprisingly, the structures with maximal symmetry, namely C_{2v} for *syn* and C_{2h} for *anti* do not correspond to the equilibrium geometry of the isolated molecules in either form. A distortion occurs in the dithiolene ligands, which are twisted away from their symmetric position. This type of distortion is present in the X-ray structures, when available, but the twist angles observed in the crystals are generally weaker than computed in the isolated molecules, with the notable exception of *anti*-$[Mo_2(\mu\text{-}S_2)S_2(S_2C_2H_4)_2]^{2-}$. Since this type of distortion is neither predicted, nor explained by means of frontier orbital interactions, but nevertheless contributes to the molecular stability by as much as 7–9 kcal mol^{-1}, it should be assigned to the relief of the strong electrostatic and Pauli repulsive interactions occurring within the coordination spheres of the two metals. Removing the $(\mu\text{-}S_2)^{4-}$ ligand abolishes the repulsive contacts and indeed restores the full symmetry. The magnitude of the repulsive interactions appears to be similar in the *syn* and *anti* forms of the same complex and do not significantly influence the energy balance. The ultimate factor conditioning the relative stability of the isomers, assumed isolated, is the overlap between the metal σ orbitals. As proposed by CLE [22], the *bent* σ bond characteristic of the *syn* form is eventually slightly more favorable than the *lateral* σ overlap encountered in the *anti* isomers and leads in most cases to a marginal stabilization of the *syn* form, comprised between 1 and 4 kcal mol^{-1}. However, the important and somewhat erratic differences noted between the observed and computed values of the dithiolene twist angle Θ suggest

that the crystal environment and more specifically the closest shell of counterions might play a prominent role in the management of the intramolecular electrostatic interactions and in the selection of the preferred isomer.

Acknowledgments

Most calculations have been carried out at the IDRIS computer center (Orsay, France), through a grant of computer time from the CNRS, and at the CURRI (ULP, Strasbourg). We are also pleased to acknowledge support from the GdR DFT.

References

[1] F. Sécheresse, E. Cadot, C. Simonnet-Jégat, in: P. Braunstein, L.A. Oro, P.R. Raithby (Eds.), Metal Clusters in Chemistry, Wiley-VCH, New-York, 1999.
[2] R.H. Holm, Chem. Soc. Rev. 10 (1981) 455.
[3] C. Zhang, G.-C. Jin, J.-X. Chen, X.-Q. Xin, K.-P. Qian, Coord. Chem. Rev. 213 (2001) 51.
[4] C. Simonnet-Jégat, E. Cadusseau, R. Dessapt, F. Sécheresse, Inorg. Chem. 38 (1999) 2335.
[5] R. Dessapt, C. Simonnet-Jégat, S. Riedel, J. Marrot, F. Sécheresse, Trans. Met. Chem. 27 (2002) 234.
[6] R. Dessapt, C. Simonnet-Jégat, F. Sécheresse, Bull. Pol. Acad. Sci., Chem. 50 (2002) 15.
[7] R. Dessapt, C. Simonnet-Jégat, A. Mallard, H. Lavanant, J. Marrot, F. Sécheresse, Inorg. Chem. 42 (2003) 6425.
[8] D. Coucouvanis, A. Hadjikyriacou, A. Toupadakis, S.-M. Koo, O. Ileperuma, M. Draganjac, A. Salifoglou, Inorg. Chem. 30 (1991) 754 (and references therein).
[9] T. Shibahara, G. Sakane, S.J. Mochida, J. Am. Chem. Soc. 115 (1993) 10408.
[10] M. Rakowski DuBois, B.R. Jagirdar, S. Dietz, B.C. Noll, Organometallics 16 (1997) 294.
[11] H. Kawaguchi, K. Yamada, J.P. Lang, K. Tatsumi, J. Am. Chem. Soc. 119 (1997) 10346.
[12] J.T. Goodman, S. Inomata, T.B. Rauchfuss, J. Am. Chem. Soc. 118 (1996) 11674.
[13] J.A. Dopke, S.R. Wilson, T.B. Rauchfuss, Inorg. Chem. 39 (2000) 5014.
[14] J.T. Goodman, T.B. Rauchfuss, J. Am. Chem. Soc. 121 (1999) 5017.
[15] J.T. Goodman, T.B. Rauchfuss, Inorg. Chem. 37 (1998) 5040.
[16] R. Dessapt, C. Simonnet-Jégat, J. Marrot, F. Sécheresse, Inorg. Chem. 40 (2001) 4072.
[17] E.I. Stiefel, Prog. Inorg. Chem. 22 (1977) 1.
[18] J.I. Gelder, J.H. Enemark, Inorg. Chem. 15 (1976) 1839.
[19] B. Spivack, Z. Dori, Coord. Chem. Rev. 17 (1975) 19.
[20] G. Bunzey, J.H. Enemark, J.K. Howie, D.T. Sawyer, J. Am. Chem. Soc. 99 (1977) 4168.
[21] G. Bunzey, J.H. Enemark, Inorg. Chem. 17 (1978) 682.
[22] T. Chandler, D.L. Lichtenberger, J.H. Enemark, Inorg. Chem. 20 (1981) 75.
[23] M.B. Hall, R.F. Fenske, Inorg. Chem. 11 (1972) 768.
[24] R. Hoffmann, W.N. Lipscomb, J. Chem. Phys. 36 (1962) 2179.
[25] R. Hoffmann, W.N. Lipscomb, J. Chem. Phys. 37 (1962) 2872.
[26] R. Hoffmann, J. Chem. Phys. 39 (1963) 1397.
[27] F. Sécheresse, private communication.
[28] J. Marrot, M.A. Pilette, F. Sécheresse, E. Cadot, Inorg. Chem. 42 (2003) 3609.
[29] Amsterdam Density Functional (ADF), User's Guide, Release 1999, Chemistry Department, Vrije Universiteit, Amsterdam, The Netherlands, 1999.
[30] E.J. Baerends, D.E. Ellis, P. Ros, Chem. Phys. 2 (1973) 41.
[31] G. Te Velde, E.J. Baerends, J. Comput. Phys. 99 (1992) 84.
[32] C. Fonseca-Guerra, O. Visser, J.G. Snijders, G. Te Velde, E.J. Baerends, in: E. Clementi, G. Corongiu (Eds.), Methods and Techniques in Computational Chemistry: METECC-95, STEF, Cagliari, Italy, 1995, pp. 305–395.
[33] A.D. Becke, J. Chem. Phys. 98 (1993) 5648.
[34] J.P. Perdew, Phys. Rev. B33 (1986) 8882.
[35] J.P. Perdew, Phys. Rev. B34 (1986) 7406.